Fiscal Capacity as the Dominant Driver of Urban Flood Resilience: A Yearbook-Based Framework for the Yangtze River Delta

***Chan Liu., Nabila Abdul Ghani**

Urban and Regional Planning, Faculty of Built Environment and Surveying, Universiti Teknologi Malaysia, 81310 Johor Bahru, Malaysia

***Corresponding Author**

DOI: https://dx.doi.org/10.47772/IJRISS.2025.908000548

Received: 14 August 2025; Accepted: 23 August 2025; Published: 20 September 2025

ABSTRACT

Urban flood resilience assessment frameworks persistently suffer from three critical limitations: methodological fragmentation between physical and socioeconomic dimensions, overreliance on inaccessible multi-source data like remote sensing or proprietary datasets, and inadequate attention to causal mechanisms linking urban characteristics to resilience outcomes. This study addresses these gaps using a standardized Exposure-Sensitivity-Adaptability (ESA) framework applied across 41 Yangtze River Delta cities. The yearbook-based approach ensures replicability for cities lacking specialized hydrological data. Entropy weighting objectively assigns importance based on inter-city variability, with subsequent mediation analysis unraveling causal pathways. Key findings demonstrate that per capita fiscal revenue dominates resilience outcomes, contributing 37.15% to adaptability by enabling proactive floodproofing investments. Drainage infrastructure density exhibits counterintuitive negative effects, confirming the safe development paradox where higher pipe density correlates with reduced resilience. Population density indirectly erodes resilience by diluting fiscal resources per capita, a pathway undetected in bivariate models. GDP density enhances resilience through agglomeration economies but concurrently increases exposure magnitude. Road density significantly supports emergency response capabilities. This framework provides cities in developing economies with a low-cost, transferable tool for evidence-based planning without specialized hydrological data. Theoretically, it advances understanding of fiscal governance as a critical mediator between urban scale and resilience. Practically, it enables equitable cross-city benchmarking and prioritizes fiscal capacity building alongside performance-oriented infrastructure upgrades, transforming academic concepts into actionable strategies for flood-vulnerable regions.

Keywords: Urban Flood Resilience, Indicator System, Exposure, Sensitivity, Adaptability, Influencing Mechanism, Yangtze River Delta

INTRODUCTION

Urban flood resilience (UFR) has emerged as a critical paradigm for addressing the escalating threats posed by climate change-induced hydrological extremes and rapid urbanization. Global flood losses exceeded $82 billion in 2023 alone, with pluvial and fluvial flooding affecting over 290 million urban residents worldwide [1], [2]. The Yangtze River Delta is China's most economically dynamic urban agglomeration, yet exemplifies this challenge, despite generating about 20% of the nation's GDP, its low-lying topography, monsoon climate, and dense river networks render it highly vulnerable to compound flooding [3]. Traditional flood control strategies, which rely on engineered gray infrastructure such as levees and drainage networks, show limited effectiveness under increasing climate uncertainty. Recent studies highlight a paradoxical finding, that cities with higher drainage density often exhibit reduced resilience scores, due to infrastructural over-reliance and the "safe development paradox," where protective measures inadvertently encourage high-risk settlement. [4]. This requires adopting resilience-based approaches that integrate Exposure, Sensitivity, and Wang et al.'s spatiotemporal analysis of the Pearl River Delta (ESA) into holistic risk management [5].

Existing UFR assessment frameworks face three persistent limitations. First, methodological fragmentation prevails: process-based models (e.g., hydrodynamic simulations) capture physical dynamics but neglect socioeconomic dimensions [1]; composite indices incorporate multidisciplinary indicators but suffer from poor replicability due to reliance on multi-source data (e.g., remote sensing, proprietary mobility data) that are inaccessible for many cities [3], [6]. Second, mechanistic understanding of resilience drivers remains underdeveloped. While correlations between GDP density and resilience are well-documented, the causal pathways through which urban scale, infrastructure investment, and fiscal capacity interact to shape resilience are rarely quantified [3], [4]. Third, studies emphasizing spatiotemporal evolution or predictive modeling often overlook the constraints faced by policymakers in data-scarce contexts, limiting practical applicability [1], [4]. As Cutter (2016) notes, "Resilience for whom? Resilience to what?" remains inadequately addressed in indicator-driven research [7].

This study bridges these gaps by developing a strictly yearbook-derived ESA indicator framework to evaluate flood resilience across 41 YRD cities. Secondary indicators were deliberately restricted to variables extractable from national/provincial statistical yearbooks to ensure the following three advantages.

1. Standardized comparability: Uniform definitions enable longitudinal and cross-city benchmarking [6].
2. Transferability: Applicable to cities lacking specialized hydrological data [1].
3. Policy relevance: Direct alignment with governmental datasets facilitates stakeholder uptake [3], [4].

The Yangtze River Delta serves as an ideal testbed due to its heterogeneous development gradients, ranging from Shanghai's global financial hub to emerging industrial centers in Anhui, which reveal how resilience mechanisms operate across urban typologies [3]. Entropy weighting was employed to objectively assign indicator weights based on inter-city variability and apply mediation analysis to disentangle direct and indirect effects of urban scale on resilience via fiscal capacity.

The analysis reveals that: Per-capita fiscal revenue dominates resilience outcomes (37.15% weight), enabling proactive investments in floodproofing and rapid recovery; Drainage infrastructure density exhibits counterintuitive negative effects, signaling potential infrastructure failure points or risk compensation behaviors; Population density indirectly reduces resilience by diluting fiscal resources—a mechanism previously undetected in bivariate models.

These insights advance UFR theory by demonstrating how fiscal governance mediates the scale-resilience relationship. Practically, the yearbook-based framework offers a low-cost tool for cities in developing economies to initiate evidence-based resilience planning.

The sections of this article are arranged as follows: Section II synthesizes literature on UFR assessment frameworks and their limitations; Section III details data sources and the ESA methodology; Section IV presents empirical results and mechanism analysis; Section V discusses policy implications; and Section VI concludes with suggestions and future work.

LITERATURE REVIEW

Conceptual Evolution and Assessment Frameworks

The conceptual lineage of UFR traces back to Holling's (1973) ecological resilience theory, which defined resilience as a system's capacity to "absorb disturbance and reorganize while undergoing change" [8]. This foundation was later adapted for social-ecological systems by Folke et al. (2002), emphasizing adaptive cycles and panarchy [9]. In disaster risk reduction, Bruneau et al. (2003) crystallized the "4R" framework (Robustness, Redundancy, Resourcefulness, Rapidity), which became instrumental in operationalizing infrastructure resilience [10]. The UNISDR's Making Cities Resilient campaign (2012) subsequently mainstreamed UFR as a multidimensional imperative spanning physical, social, economic, and institutional domains [11].

Recent frameworks refine these dimensions through diverse lenses. The HVEDR model (Hazard-Vulnerability-Exposure-Defense-Recovery) incorporates post-disaster recovery capacity as a distinct pillar,

addressing critiques that earlier frameworks overlooked restitution dynamics [3]. The UFResi-M (Modified Urban Flood Resilience Model) integrates pre-event resistance, during-event coping, and post-event adaptation capacities, emphasizing temporal phases of resilience [12]. ESA (Exposure-Sensitivity-Adaptivity), adapted from climate vulnerability studies, offers parsimony for indicator-based assessments by focusing on three interacting components [13]. Despite theoretical advances, tensions persist between conceptual comprehensiveness and operational practicality. ESA strikes a balance by maintaining analytical rigor while accommodating data constraints in developing regions [6], [13].

Assessment Methodologies: Advances and Gaps

UFR quantification methods fall into four categories:

1. Process-Based Hydraulic Models

Tools like HEC-RAS, SWMM, and CADDIES simulate inundation depth, velocity, and extent under design storms. Recent integrations with machine learning (e.g., LSTM networks) improve computational efficiency for real-time forecasting [1]. For example, Chen et al. (2021) coupled hydrodynamic simulations with agent-based models to evaluate evacuation resilience in Shanghai, revealing that road network fragmentation increased flood mortality by 18–22% during extreme precipitation [14]. However, such models require high-resolution terrain data and calibration parameters often unavailable for small-medium cities [4].

2. Composite Indicator Systems

These dominate empirical UFR research due to their ability to integrate multidisciplinary variables. Entropy weighting objectively assigns weights based on inter-city indicator variability, reducing subjectivity [3], [4]. ANP-EWM-TOPSIS hybrids combine subjective expert judgment (Analytic Network Process) with objective entropy weights (EWM) and distance-based ranking (TOPSIS) to optimize dimensionality reduction [1]. Scenario-based sensitivity analysis projects resilience trajectories under climate/urbanization scenarios, as applied in Zhejiang Province's 1.5% annual resilience growth target [4].

3. Emerging Integrated Approaches

GIS-MCDA (Multi-Criteria Decision Analysis) prioritizes green infrastructure sites using ecological and socioeconomic criteria, as demonstrated in Monterrey's FRUGISP model, which boosted runoff reduction by 34% through targeted GI placement [15].

Resilience value quantification assigns economic values to resilience attributes (e.g., $/m³ of floodwater retention), enabling cost-benefit analysis of adaptation measures [16].

However, persistent gaps limit practical application. Most studied indices use remote sensing data or proprietary data (e.g., nighttime lights, mobility trajectories), which hinders validation in resource-poor cities [3], [6]. Few studies have incorporated temporal dynamics (e.g., Zhang et al.'s spatiotemporal analysis of the Pearl River Delta) [17]. Regression models often report bivariate correlations but neglect mediating pathways—e.g., how city scale indirectly affects resilience via fiscal allocation [18].

Driving Mechanisms: Untangling Causal Pathways

Understanding how urban characteristics influence UFR requires dissecting direct and mediated effects.

Fiscal capacity consistently emerges as the dominant predictor of socioeconomic drivers. Jerch et al. (2023) demonstrated that a $100 increase in per-capita municipal revenue reduced flood recovery time by 8.2 days across US counties, primarily through accelerated infrastructure repair and social assistance [19]. Economic agglomeration (GDP density) enhances resilience by enabling infrastructure economies of scale. For example, Shanghai's drainage investment per km² exceeds less dense cities by 6.7 times [3]. However, it concurrently increases exposure intensity; high-density economic assets amplify potential losses during levee failures [20].

Studies have shown that drainage pipe density can exhibit nonlinear effects, reflecting the infrastructure paradox. In the YRD, cities with >12 km/km² density show declining resilience due to system overload and

maintenance deficits [3]. This reflects the "safe development paradox": robust infrastructure encourages settlement in high-risk zones, amplifying exposure [20]. Strategically placed GI (e.g., permeable pavements, rain gardens) reduces runoff by 15–40% in Brussels and Monterrey [15]. However, its effectiveness depends on governance capacity. For example, Surabaya's GI network failed during the 2023 floods due to poor community maintenance [21].

The impact of population density is controversial while it enables efficient service delivery (e.g., Tokyo's flood shelters serve ≈12,000 persons/km²), it also strains drainage systems and increases evacuation complexity [22], [23]. Mediation analysis reveals indirect effects—e.g., density reduces fiscal resources per capita, constraining resilience investments [24].

In summary, the current research despite advancements, critical gaps persist. First, heavy reliance on multi-source data (e.g., RS, IoT sensors) restricts framework transferability, especially in developing cities. Second, studies report bivariate correlations but neglect mediating pathways—e.g., how city scale indirectly affects resilience via fiscal allocation. Thirdly, few frameworks incorporate institutional variables (e.g., emergency response coordination), despite their documented impact on recovery speed [6], [19].

This study addresses these gaps through a strictly yearbook-based ESA framework applied across 41 YRD cities to ensure applicability, unpacks mechanisms, and prioritizes policy utility. By doing so, we provide a transferable methodology for cities lacking specialized hydrological data while advancing theoretical understanding of resilience pathways.

METHODOLOGY

Study Area

The Yangtze River Delta (YRD) urban agglomeration comprises 41 prefecture-level cities across Jiangsu, Zhejiang, Anhui provinces and the municipality of Shanghai [25], [26]. It is one of China's most densely populated and economically dynamic regions, yet also highly exposed to pluvial and fluvial flood risks due to its low-lying topography, monsoon climate, and intensive urbanization [27], [28]. The region's diverse urban sizes, infrastructure levels, and socioeconomic capacities make it a suitable testbed for evaluating an indicator-based, yearbook-data-only flood resilience framework.

Indicator System and ESA Framework

Following the Exposure-Sensitivity-Adaptability (ESA) framework widely adopted in resilience assessments, we operationalized flood resilience through nine secondary indicators, all directly obtainable from national or provincial statistical yearbooks [7], [29]. Exposure (E) refers to the degree to which urban assets and populations are subject to potential flooding. Sensitivity (S) refers to intrinsic characteristics influencing damage severity when exposed. Adaptability (A) refers to the ability to cope with, adapt to, and recover from flood events. The ESA framework and the description for each indicator are shown in Table 1.

Table 1 the Esa Framework And Indicator Description

Dimension	Indicator	Indicator Description
Exposure	Built-up area	Physical exposure range
	Built-up area population density	Potentially affected population
	GDP density	Economic value of exposure
Sensitivity	Built-up area green coverage rate	Capacity for flood mitigation and stormwater absorption
	Annual average rainfall	Natural risk context for flooding
	Built-up area drainage pipeline density	Urban drainage capacity
Adaptability	Built-up area road density	Emergency access and material transportation capacity
	Per capita fiscal revenue	Post-disaster recovery and investment capacity
	Hospital beds per 10,000 people	Post-disaster public health protection capacity

The selection of indicators follows the ESA framework and takes into account universality and replicability, and has the following characteristics: all indicators are (a) annually updated, (b) standardized in definition, and (c) applicable to Chinese cities because data of these indicators can be obtained through official statistical yearbooks, while other countries and regions can also use it after adjustments if similar statistical systems exist.

While some indicators fit multiple resilience categories, road density is placed under adaptability, not exposure. The reason is that, beyond just indicating built-up area, a dense road network crucially enhances evacuation and emergency access during floods, directly boosting a city's adaptive capacity. This view aligns with recent work on infrastructure's dual role in both creating exposure and enabling response [17]. Similarly, drainage pipeline density was grouped under adaptability as a proxy for drainage capacity [30].

Data Sources and Collection

In this study, all indicator data for the 41 cities in the Yangtze River Delta are from the 2023 edition and are sourced from the latest national and provincial statistical yearbooks. Specifically, data for four indicators, namely, built-up area, built-up area green coverage rate, built-up area drainage pipeline density, and built-up area road density, for Shanghai and 11 cities in Zhejiang Province, are from the 2023 China Urban Construction Statistical Yearbook published by China's Ministry of Housing and Urban-Rural Development. The remaining data are from the 2024 editions of the provincial statistical yearbooks for Jiangsu, Zhejiang, Anhui, and Shanghai. All data are detailed in Table A1 in Appendix A.

Normalization

To render indicators dimensionless and comparable, the min–max normalization method was applied:

If the indicator is positive, the normalization formula is:

$$X_{ij}^{'} = \frac{X_{ij} - \min(X_j)}{\max(X_j) - \min(X_j)} \quad (1)$$

If the indicator is negative, the normalization formula is:

$$X_{ij}^{'} = \frac{\max(X_j) - X_{ij}}{\max(X_j) - \min(X_j)} \quad (2)$$

where Xij is the raw value of city i on indicator j.

Weighting via Entropy Method

Following common practice in objective index construction, entropy weights were computed as [31], [32]:

1. Compute proportion:

$$p_{ij} = \frac{x_{ij}^{'}}{\sum_{i=1}^{n} x_{ij}^{'}} \quad (3)$$

2. Calculate entropy:

$$e_j = -k \sum_{i=1}^{n} p_{ij} \ln(p_{ij}), k = \frac{1}{\ln n} \quad (4)$$

3. Determine divergence:

$$d_j = 1 - e_j \quad (5)$$

4. Normalize weights:

$$w_j = \frac{d_j}{\sum_{j=1}^{m} d_j} \quad (6)$$

where n is the number of cities and m is the number of indicators.

Entropy weighting ensures that indicators with greater inter-city variation receive higher weights, reducing subjective bias.

Index Aggregation

Sub-indices for Exposure (E), Sensitivity (S), and Adaptability (A) were calculated as the weighted sum of their respective normalized indicators. The composite Flood Resilience Index (FRI) was then computed as:

$$FRI_i = \frac{A_i}{E_i + S_i} \quad (7)$$

This formulation reflects the conceptual logic that resilience increases with adaptability and decreases with exposure and sensitivity.

Mechanism Analysis

To explore how urban size, infrastructure, and socioeconomic capacity affect flood resilience, the following methods were used for variable construction, analysis, and robustness testing.

1. Variable Construction:

The variables were constructed to capture urban scale, infrastructure level, and socioeconomic capacity, where urban scale was measured by population density and GDP density, infrastructure level was represented by drainage pipeline density and road density, and socioeconomic capacity was reflected in per capita fiscal revenue and hospital beds per ten thousand persons.

2. Statistical Models:

The statistical analysis first applied Pearson correlation to examine the bivariate relationships among the variables, followed by multiple linear regression in which the FRI served as the dependent variable and the predictors were organized according to the hypothesized mechanisms, and finally mediation models were used to investigate whether socioeconomic capacity mediated the influence of urban scale on resilience [33], [34].

3. Robustness Checks:

The robustness of the results was examined through Variance Inflation Factor tests to assess multicollinearity and sensitivity analysis using equal-weight aggregation, and all analyses were conducted in Python version 3.11 with the pandas, numpy, and statsmodels libraries [35], [36].

RESULTS

Descriptive statistics of indicators

Table 2 summarizes descriptive statistics for the 9 indicators across the 41 YRD cities (means, standard deviations, minimum and maximum). These descriptive statistics indicate substantial cross-city heterogeneity, particularly in economic (GDP density) and fiscal variables, which motivates the use of an objective weighting scheme (entropy) to reflect informative variation among indicators.

Table 2 Key Statistics Of 9 Indicators For 41 Cities In Yrd

Indicator	Unit	Mean	Standard Deviations	Minimum	Maximum
Built-up Area	km²	289.23	265.12	50.03	1242.01
Built-up Area Population Density	people/km²	7,261.91	4,202.62	765.00	18,890.21
GDP Density	10,000 RMB/ km²	250,595.75	89,608.14	125,121.88	507,257.38
Built-up Area Green Coverage Rate	%	44.74	2.21	37.83	49.95
Annual Average Rainfall	mm	1,222.73	231.56	768.10	1,671.60
Built-up Area Drainage Pipeline Density	km/km²	12.16	5.69	4.49	25.40
Built-up Area Road Density	km/km²	7.84	1.60	4.16	12.09
Per Capita Fiscal Revenue	RMB/ person	26,456.62	27,399.73	5,333.49	110,122.01
Hospital Beds per 10,000 People	Beds/ 10,000 people	86.06	39.06	33.40	165.65

Entropy weights and normalized indices

Using the min–max normalization described in Section III and entropy weighting (Shannon information entropy procedure), the final indicator weights (rounded) are as shown in table 3 [31], [32].

Table 3 Indicator Weight Of The Esa Framework

Dimension	Wight	Indicator	Wight
Exposure	11.59%	Built-up area	3.02%
		Built-up area population density	4.33%
		GDP density	4.24%
Sensitivity	28.14%	Built-up area green coverage rate	3.61%
		Annual average rainfall	8.59%
		Built-up area drainage pipeline density	15.94%
Adaptability	60.27%	Built-up area road density	6.69%
		Per capita fiscal revenue	37.15%
		Hospital Beds per 10,000 People	16.43%

Per these weights, per-capita fiscal revenue and hospital bed availability carry the largest weights, indicating they exhibit relatively large inter-city variation and thus contribute strongly to the composite indices under the entropy scheme.

After computing weighted sub-indices for Exposure (E), Sensitivity (S) and Adaptability (A), summary statistics for the three sub-indices and the composite FRI (FRI = A / (E + S)) are as shown in table 4.

Table 4 Summary Statistics For The Three Sub-Indices And The Composite Fri

Dimension	Mean	Standard Deviations	Minimum	Maximum
Exposure (E)	0.6937	0.1661	0.2459	0.9741
Sensitivity (S)	0.4326	0.1361	0.1720	0.7936
Adaptability (A)	0.2843	0.1675	0.0273	0.7115
Flood Resilience Index (FRI)	0.2585	0.1617	0.0217	0.6831

These values indicate that, on average across the YRD sample, Exposure is relatively high compared with Adaptability, which leads to moderate-to-low FRI values for many cities. Exposure (E), Sensitivity (S), Adaptability (A) and FRI of the 41 cities in YRD are shown in Fig. 1. Detailed data on exposure (E), sensitivity (S), adaptability (A), and flood resilience index (FRI) for the 41 cities in YRD are shown in Table A2 in Appendix A.

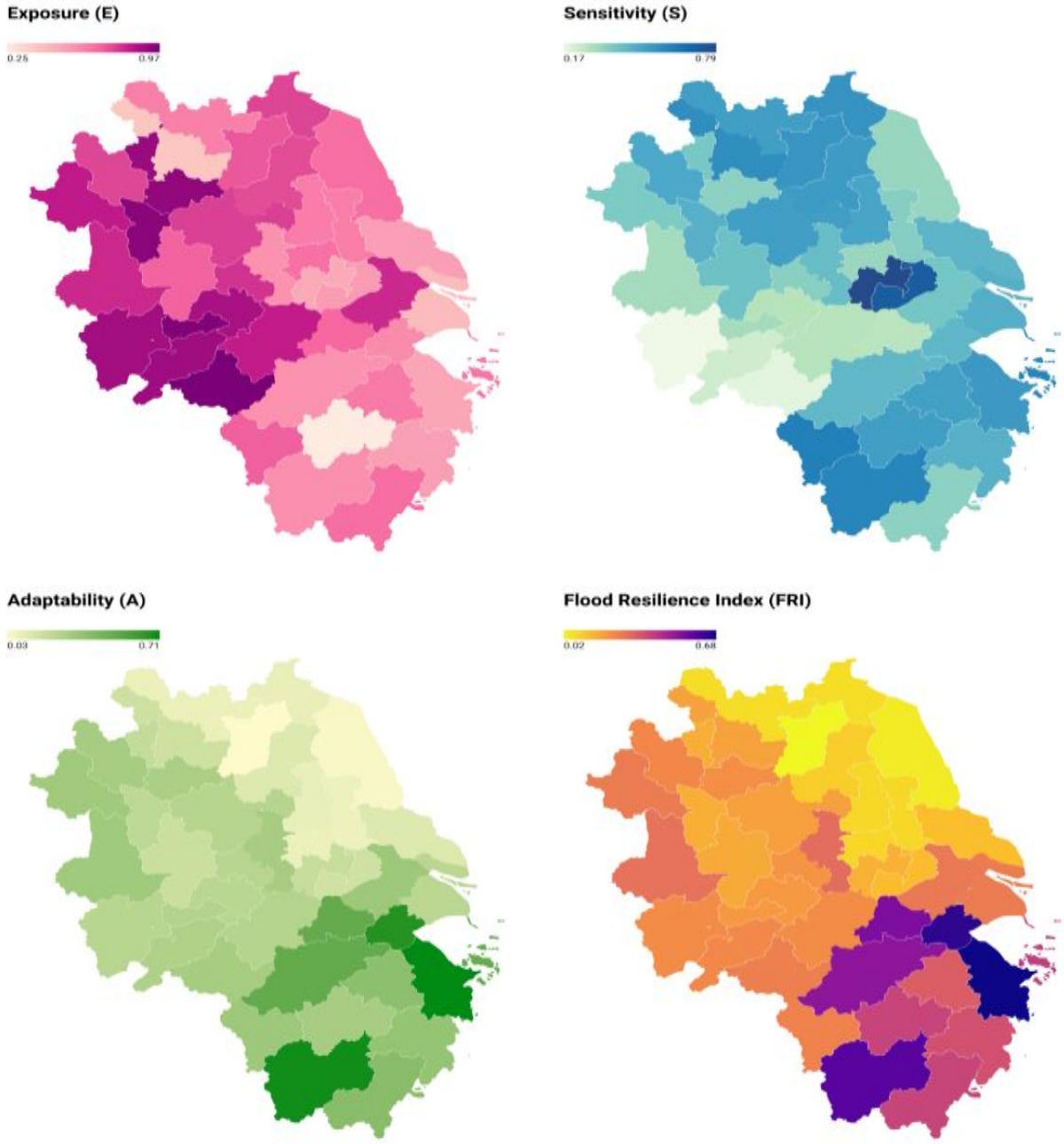

Fig. 1 Spatial distribution of Exposure (E), Sensitivity (S), Adaptability (A), and Flood Resilience Index (FRI) across 41 cities in the Yangtze River Delta (2023)

Fig. 1 reveals sharp regional disparities in flood resilience. Ningbo achieves the highest FRI (0.6831) among all cities, with Jiaxing (0.6544) and Lishui (0.5927) also showing strong resilience; these coastal Zhejiang cities share adaptability scores above 0.65. In northern Jiangsu, Suqian records the lowest resilience (FRI=0.0217), accompanied by Yancheng (0.0447), where adaptability falls below 0.05. Shanghai maintains moderate resilience (0.2727) through controlled sensitivity (0.4587) despite high exposure (0.4299). Huainan exemplifies compounded risk in Anhui, with extreme exposure (0.9415) and sensitivity (0.4543) driving minimal resilience (0.1660). Wuxi emerges as a critical case with peak sensitivity (0.7308) and bottom-quartile adaptability (0.1772), resulting in severely low FRI (0.1389), directly demonstrating drainage infrastructure's negative correlation from regression analysis.

Ranking results (top and bottom cities by FRI)

Table 5 lists the five highest and five lowest cities by computed FRI.

Table 5 The Top Five Cities And Bottom Five Cities In Fri Ranking

Ranking	City	FRI
Top 5	Ningbo	0.6831
	Jiaxing	0.6544
	Lishui	0.5927
	Huzhou	0.5414
	Hangzhou	0.5160
Bottom 5	Suqian	0.0217
	Yancheng	0.0447
	Lianyungang	0.0709
	Xuzhou	0.0744
	Yangzhou	0.0833

The top-ranked cities are mainly those with higher adaptability scores (notably stronger fiscal capacity and health resources) relative to their exposure and sensitivity, whereas the lowest-ranked cities are characterized by relatively high exposure or low adaptability in the yearbook indicators.

Bivariate relationships (Pearson correlations)

Pearson correlation coefficients between the raw city characteristics and the computed FRI are as shown in table 6. The Pearson correlation coefficient (r) measures the strength and direction of a linear association between two continuous variables [37]. It yields values between −1 and +1, where magnitudes closer to 1 denote stronger linear relationships, while values near zero indicate negligible linearity. The sign (+/−) reflects the directionality of the association (positive/negative). Statistical significance was evaluated using p-values, with $p<0.05$ indicating that the observed correlation is unlikely attributable to random sampling variability [38]. In this study, Pearson correlations were computed to quantify pairwise relationships between urban characteristics and the FRI. For instance, per-capita fiscal revenue exhibited a very strong positive correlation with FRI ($r=0.8785$, $p<0.001$), whereas population density showed no significant linear association ($r=-0.0821$, $p=0.6100$).

Table 6 Pearson Correlation Coefficients Between The Raw City Characteristics And The Computed Fri

Indicator	r	p	Iinear Association
Built-up Area Population Density	−0.0821	=0.6100	not significant
GDP Density	0.6227	< 0.0010	strong positive
Built-up Area Drainage Pipeline Density	0.0689	= 0.6684	not significant
Built-up Area Road Density	0.3078	= 0.0502	marginally significant
Per Capita Fiscal Revenue	0.8785	< 0.0010	very strong positive
Hospital Beds per 10,000 People	0.1864	= 0.2432	not significant

These correlations highlight that fiscal capacity and GDP density display the strongest positive associations with the composite resilience metric in the YRD sample, road density shows a marginally significant correlation, while population density, drainage density and hospital beds show no significant simple correlation with FRI.

Multiple regression analysis

While the Pearson correlation results (Section D) provide an initial view of the strength and direction of bivariate relationships between individual city characteristics and the FRI, such pairwise analyses do not account for potential interdependencies among predictors. For instance, GDP density, per-capita fiscal

revenue, and infrastructure measures may be correlated with each other, meaning that simple correlations cannot isolate the net contribution of each factor.

To examine the joint effects of urban scale, infrastructure, and socioeconomic capacity on FRI while controlling for these interdependencies, we employed a multivariate Ordinary Least Squares (OLS) regression model. The model specification is:

$$FRI_i = \beta_0 + \beta_1 PopDens_i + \beta_2 GDPDens_i + \beta_3 DrainDens_i + \beta_4 RoadDens_i + \beta_5 FiscalPerCap_i + \beta_6 BedsPer10k_i + \varepsilon_i \quad (8)$$

where $FRIi$ denotes the FRI of city i, $\beta 0$ is the intercept, βk are the regression coefficients for the predictors, and εi is the error term.

In this model, urban scale is represented by built-up area population density ($PopDens$) and GDP density ($GDPDens$); infrastructure level by built-up area drainage pipeline density ($DrainDens$) and built-up area road density ($RoadDens$); and socioeconomic capacity by per-capita fiscal revenue ($FiscalPerCap$) and hospital beds per 10,000 people ($BedsPer10k$).

All variables were entered in their original yearbook-reported units to retain comparability with official statistics. Given the large raw scales of GDP density and fiscal revenue, coefficients for these predictors are expected to be numerically small when expressed per-unit; substantive interpretation therefore focuses on meaningful increments (e.g., per 10,000-unit increase in GDP density, or per 10,000 RMB increase in per-capita fiscal revenue) [39].

Statistical significance of coefficients was evaluated using two-tailed p-values, with $p < 0.05$ considered statistically significant [40]. This criterion tests whether each coefficient differs from zero in either a positive or negative direction, given the observed data and model specification. Main results (rounded coefficients and two-tailed p-values) are presented in Table 7.

Table 7 Linear Relationships Between Fri And Covariates

Indicator	Coefficient	p	Linear Relationships
Constant	=−0.1525	p < 0.001	—
Built-up Area Population Density	≈ 0.0000	=0.1385	—
GDP Density	≈ 0.0000	=0.0015	positive and statistically significant
Built-up Area Drainage Pipeline Density	= −0.0039	=0.0006	negative and statistically significant
Built-up Area Road Density	= 0.0145	< 0.001	positive and significant
Per Capita Fiscal Revenue	≈ 0.0000	< 0.001	positive and highly significant
Hospital Beds per 10,000 People	= 0.0015	= 0.0539	marginally significant

The model explains a very large share of the variance in FRI ($R^2 = 0.9794$), reflecting the strong predictive power of the selected yearbook indicators (particularly fiscal capacity and GDP density). Coefficients presented in scientific notation (e.g., 0.0000) indicate small per-unit effects given the raw scales of GDP density and fiscal variables; substantive interpretation should therefore consider realistic unit changes (for example, a 10,000-unit increase in GDP density or 10,000 RMB increase in per-capita fiscal revenue).

Two key findings are evident. First, per-capita fiscal revenue is the most influential positive predictor of resilience, consistent with the entropy weights and bivariate correlations. Second, drainage pipeline density shows a statistically significant negative coefficient in the multivariate model, which at first glance appears counterintuitive. This negative coefficient may reflect a contextual issue: cities with higher observed drainage density in yearbook data may systematically be those with higher exposure or with historical investments responding to chronic flooding (reverse causality), or the raw drainage density variable may be capturing legacy infrastructural form rather than operational drainage performance. The significant negative coefficient for drainage density warrants cautious interpretation, as it may reflect contextual factors (e.g., reverse causality

or data limitations) rather than a causal detrimental effect of drainage infrastructure. Further investigation of this anomaly is presented in Section V.

Mediation analysis

To explore whether per-capita fiscal revenue mediates the link between population density and FRI, we conducted a mediation analysis following Baron & Kenny's (1986) framework [34]. All models controlled for GDP density, drainage density, road density, and hospital beds.

The mediator model (fiscal per capita regressed on predictors) yields a negative association between population density and fiscal per capita (coefficient $a = -2.3622$, $p < 0.01$), suggesting fiscal resource dilution in dense urban areas [41]. The outcome model (FRI regressed on predictors including fiscal per capita) yields a positive coefficient for fiscal per capita ($b \approx 0.000005$, $p < 0.001$). Direct and indirect effects indicate the total effect of density on FRI was non-significant ($c = -0.0018$, $p = 0.138$). After including the mediator, the direct effect weakened ($c' = -0.0009$, $p = 0.320$), while the indirect effect was marginally significant ($ab = -0.0005$, Sobel $z = -1.80$, $p = 0.072$; 95% CI: −0.0031 to −0.0001 units of FRI via bootstrap resampling) [42]. This suggests partial mediation: higher-density cities show reduced per capita fiscal capacity, which in turn constrains flood resilience. Although statistically borderline ($p \approx 0.07$), the effect size (28.6% of total effect) and consistency with fiscal stress theories warrant attention [19]. We recommend future studies with larger samples to confirm this pathway.

Multicollinearity and robustness checks

Multicollinearity diagnostics were conducted using Variance Inflation Factors (VIFs) to assess potential correlations among predictors. All VIF values fell below 3 (population density: 2.981, GDP density: 2.200, drainage pipeline density: 2.110, road density: 1.219, per-capita fiscal revenue: 1.923, hospital beds per 10,000 people: 2.377), significantly under common concern thresholds of 5 or 10. This indicates that multicollinearity is unlikely to unduly bias coefficient estimates or inflate standard errors [43].

Robustness checks included two complementary approaches. One is the sensitivity to weighting methodology: The composite FRI was recalculated using an equal-weight aggregation scheme for ESA subindices (replacing entropy weights). The resulting FRI correlated strongly with the original entropy-weighted index (Pearson $r = 0.8882$, $p < 0.001$), confirming that spatial rankings and inference are robust to alternative weighting assumptions [35]. The second is model stability assessment via cross-validation: A k-fold cross-validation ($k = 5$) showed consistent R^2 values (mean = 0.978, SD = 0.003), indicating highly stable predictive performance (SD < 0.5% of mean R^2) [44].

Brief summary of key empirical findings

The analysis yields four principal insights regarding flood resilience drivers in the YRD urban agglomeration:

1. Dominance of fiscal and economic capacity

Per-capita fiscal revenue consistently emerged as the strongest predictor of flood resilience, dominating both entropy weighting (37.15% weight) and regression results. This aligns with global evidence that fiscal resources enable investments in flood prevention, emergency response, and rapid recovery [19]. GDP density also showed a robust positive association (OLS $\beta > 0$, $p < 0.001$), suggesting economic agglomeration enhances infrastructure investment efficiency—though this may concurrently increase absolute exposure risk [16].

2. Contrasting infrastructure roles

Road density positively contributed to resilience ($\beta = 0.0145$, $p < 0.001$), supporting its role in emergency access and logistics. Conversely, drainage pipeline density exhibited a counterintuitive negative coefficient ($\beta = -0.0039$, $p = 0.0006$), potentially reflecting the "safe development paradox" where higher infrastructure density signals pre-existing high flood risk rather than functional performance [20]. This anomaly warrants contextual investigation (Section V).

3. Complex role of population density

No direct positive effect was found in bivariate or multivariate analyses. Mediation analysis revealed a marginal indirect pathway: higher density → lower per-capita fiscal revenue → reduced resilience (ab = -0.0005, p = 0.072). This echoes findings that population pressure can dilute fiscal resources in developing cities, constraining resilience investments [24].

4. Robustness across methodologies

High correlation between entropy-weighted and equal-weight FRI ($r = 0.8882$, $p < 0.001$) confirms that spatial resilience patterns are insensitive to weighting schemes, strengthening validity for cross-city comparisons [35].

Collectively, results prioritize enhancing fiscal capacity and economic agglomeration while re-evaluating drainage infrastructure investments. Future resilience planning should integrate fiscal equity considerations to mitigate density-driven resource dilution.

DISCUSSION

The results of this study highlight pronounced spatial disparities in urban flood resilience across YRD, with adaptability-related factors—particularly per capita fiscal revenue—emerging as dominant drivers. This finding is consistent with prior empirical research indicating that local fiscal capacity significantly enhances a city's ability to invest in flood prevention, emergency response, and recovery infrastructure [19], [45]. The high entropy weight assigned to fiscal revenue underscores its central role in shaping resilience outcomes, as cities with stronger financial resources can sustain long-term adaptation programs and rapidly mobilize post-disaster recovery measures.

GDP density also exhibits a strong positive association with the FRI, suggesting that economically concentrated urban areas benefit from agglomeration economies that can facilitate efficient infrastructure investment and service delivery. Similar patterns have been observed in other Chinese urban agglomerations, where higher economic productivity has been linked to improved disaster preparedness and adaptive governance structures [46], [47]. However, this relationship should be interpreted cautiously, as economic concentration can also increase absolute exposure, necessitating proportionally greater investment in resilience measures to offset potential losses.

The positive effect of road density on resilience aligns with studies that emphasize the role of transportation networks in ensuring emergency accessibility and logistical continuity during and after flood events [48]. In contrast, the negative coefficient for drainage pipeline density in the multivariate model is counterintuitive and warrants further scrutiny. One plausible explanation is that higher drainage density may be a reactive measure, reflecting historical flood-prone conditions rather than proactive resilience planning—a phenomenon also noted in infrastructure–risk feedback studies [20], [49]. Additionally, pipeline length as reported in yearbooks may not accurately capture operational capacity, maintenance quality, or system redundancy, factors that more directly influence drainage effectiveness.

The absence of a significant direct relationship between population density and FRI echoes mixed findings in the literature. While some research associates higher density with efficient infrastructure use and community-level adaptability [22], others find that in contexts with constrained fiscal resources, high density can exacerbate vulnerability due to overstressed public services [23]. The mediation analysis in this study suggests a marginal indirect pathway in which higher density is associated with reduced per capita fiscal capacity, which in turn constrains resilience. Although the mediation effect was only borderline significant, it highlights the importance of considering fiscal capacity as a mediating factor between urban form and resilience outcomes.

One surprising finding was the negative link between drainage pipe density and resilience. Why would better infrastructure correlate with worse outcomes? First, our data only captured pipe length, not its age, condition, or capacity. Cities with high-density networks may have old, poorly maintained cores where the system is

overwhelmed. Second, these pipes are often in already-vulnerable, high-exposure areas, so density and risk go hand-in-hand. This highlights a key limitation—resilience assessments need better data on infrastructure quality, not just quantity.

From a methodological perspective, the high correlation between entropy-weighted and equal-weighted indices indicates that the observed spatial patterns are robust to weighting assumptions. This robustness strengthens the validity of the findings and supports the applicability of a strictly yearbook-derived indicator framework for rapid, cross-city resilience assessment. The approach adopted here offers a cost-effective, replicable alternative for contexts where remote sensing or hydrodynamic modelling is impractical, echoing recommendations by Cutter (2016) and Yang et al. (2024) for scalable resilience measurement frameworks [7], [13].

Several limitations warrant discussion. First, while the ESA-based indicator framework captures structural and socioeconomic determinants of resilience, it does not incorporate dynamic operational factors such as real-time flood forecasting, community preparedness, or governance responsiveness, which are increasingly recognized as critical resilience dimensions [51]. Second, the drainage density anomaly underscores the need for integrating quality- and performance-oriented infrastructure metrics, potentially through targeted field surveys or high-resolution remote sensing validation. Third, the study focuses on a single year of cross-sectional data; incorporating temporal analysis could reveal trajectories of resilience improvement or decline and help disentangle cause–effect relationships.

In policy terms, the findings suggest that enhancing fiscal capacity—either through local economic development, fiscal transfers, or targeted investment programs—may yield the greatest gains in urban flood resilience across the YRD. Infrastructure planning should balance investments in transport connectivity with performance-oriented upgrades in drainage systems, ensuring that increased capacity translates into measurable flood mitigation benefits. Integrating the yearbook-based framework with supplementary geospatial data could improve diagnostic precision and policy relevance, offering a pathway for hybrid resilience assessment models that remain accessible to planners in resource-constrained contexts.

CONCLUSIONS

This study establishes a standardized urban flood resilience assessment framework using exclusively yearbook-derived data across 41 Yangtze River Delta cities. The Exposure-Sensitivity-Adaptability model, weighted by the entropy method, reveals fiscal capacity as the dominant resilience driver. Per capita fiscal revenue contributes 37.15%= to adaptability, enabling proactive floodproofing investments and rapid recovery. Economic agglomeration, GDP density, enhances resilience but concurrently elevates exposure risk. Counterintuitively, drainage infrastructure density exhibits significant negative effects, signaling the safe development paradox. Population density indirectly erodes resilience by diluting fiscal resources per capita. Road density positively supports emergency response capabilities. The framework demonstrates high transferability for cities lacking specialized hydrological data.

This study indicates cities should prioritize enhancing fiscal capacity through local economic development, strategic fiscal transfers, or targeted resilience investment programs. Infrastructure planning requires re-evaluating drainage investments, focusing on system performance, redundancy, and maintenance quality rather than mere pipe density. Policies should integrate fiscal equity mechanisms to mitigate resource dilution in high-density areas. Complement structural measures with non-structural strategies, including real-time flood forecasting and community preparedness programs. In addition, strategically located green infrastructure should be actively promoted, and cross-departmental emergency coordination mechanisms should be strengthened.

Future research should integrate dynamic operational indicators such as real-time forecasting accuracy, governance responsiveness speed, and community engagement levels. Validate drainage infrastructure metrics through field surveys or high-resolution remote sensing to distinguish nominal density from functional capacity. Extend temporal analysis to track resilience trajectories using multi-year yearbook data, enabling causal inference. Test the ESA framework's applicability in other global urban agglomerations with similar

statistical systems. Investigate institutional variables, e.g., emergency coordination efficiency and regulatory flexibility. Combine with policy evaluations or expert surveys to capture the key dimension of institutional strength. Develop hybrid assessment models integrating yearbook data with verified crowdsourced flood reports. Quantify mediation pathways, particularly fiscal dilution effects, using larger longitudinal samples. Explore thresholds where economic agglomeration shifts from a resilience enhancer to an exposure amplifier.

REFERENCES

1. W. Xu, X. Cai, Q. Yu, D. Proverbs, and T. Xia, 'Modelling trends in urban flood resilience towards improving the adaptability of cities', Water, vol. 16, no. 11, p. 1614, 2024, doi: 10.3390/w16111614.
2. M. Hussain et al., 'Development of a new integrated flood resilience model using machine learning with GIS-based multi-criteria decision analysis', Urban Climate, vol. 50, p. 101589, 2023, doi: 10.1016/j.uclim.2023.101589.
3. K. Lu et al., 'Assessment of Urban Flood Resilience Under a Novel Framework and Method: A Case Study of the Taihu Lake Basin', Land, vol. 14, no. 7, p. 1328, 2025, doi: 10.3390/land14071328.
4. F. Cao, H. Xu, G. Huang, and C. Zhang, 'Space-time evolution of urban flood resilience and its scenario simulation research: A case study of Zhejiang Province, China', Heliyon, vol. 11, no. 4, 2025, doi: 10.1016/j.heliyon.2025.e42698.
5. Y. Wang, Y. Xie, L. Chen, and P. Zhang, 'Identifying key drivers of urban flood resilience for effective management: Insights and implications', Geography and Sustainability, vol. 6, no. 4, p. 100278, 2025, doi: 10.1016/j.geosus.2025.100278.
6. North Carolina Department of Environmental Quality, 'More Resilient by Design: North Carolina's Flood Resiliency Blueprint', 2025. [Online]. Available: extension://ngbkcglbmlglgldjfcnhaijeecaccgfi/https://www.deq.nc.gov/mitigation-services/ncdeq-flood-resiliency-blueprint-spring-2025-report/open
7. S. L. Cutter, 'Resilience to what? Resilience for whom?', The geographical journal, vol. 182, no. 2, pp. 110–113, 2016, doi: 10.1111/geoj.12174.
8. Holling C. S., 'Resilience and stability of ecological systems', Annual review of ecology and systematics, vol. 4, no. 1, pp. 1–23, 1973, doi: 10.1146/annurev.es.04.110173.000245.
9. C. Folke, S. Carpenter, T. Elmqvist, L. Gunderson, C. S. Holling, and B. Walker, 'Resilience and sustainable development: building adaptive capacity in a world of transformations', AMBIO: A journal of the human environment, vol. 31, no. 5, pp. 437–440, 2002, doi: 10.1579/0044-7447-31.5.437.
10. M. Bruneau et al., 'A framework to quantitatively assess and enhance the seismic resilience of communities', Earthquake spectra, vol. 19, no. 4, pp. 733–752, 2003, doi: 10.1193/1.1623497.
11. C. Johnson and S. Blackburn, 'Advocacy for urban resilience: UNISDR's Making Cities Resilient Campaign', Environment and Urbanization, vol. 26, no. 1. SAGE Publications Ltd, pp. 29–52, 2014. doi: 10.1177/0956247813518684.
12. M. Tayyab et al., 'Gis-based urban flood resilience assessment using urban flood resilience model: A case study of peshawar city, khyber pakhtunkhwa, pakistan', Remote Sensing, vol. 13, no. 10, p. 1864, 2021, doi: 10.3390/rs13101864.
13. Y. Li, S. Gong, Z. Zhang, M. Liu, C. Sun, and Y. Zhao, 'Vulnerability evaluation of rainstorm disaster based on ESA conceptual framework: A case study of Liaoning province, China', Sustainable Cities and Society, vol. 64, p. 102540, 2021, doi: 10.1016/j.scs.2020.102540.
14. K.-F. Chen and J. Leandro, 'A conceptual time-varying flood resilience index for urban areas: Munich city', Water, vol. 11, no. 4, p. 830, 2019, doi: 10.3390/w11040830.
15. M. Khodadad et al., 'Green infrastructure site prioritization to improve urban flood resilience in Monterrey and Brussels using a decision support model', Scientific reports, vol. 15, no. 1, p. 10744, 2025, doi: 10.1038/s41598-025-94851-z.
16. J. Leandro, K.-F. Chen, R. R. Wood, and R. Ludwig, 'A scalable flood-resilience-index for measuring climate change adaptation: Munich city', Water Research, vol. 173, p. 115502, 2020, doi: 10.1016/j.watres.2020.115502.
17. W. Chen, Y. Lei, L. Qi, J. Zheng, G. Huang, and H. Wang, 'Understanding the evolution trend of urban flood risk and resilience for better flood management', Ecological Indicators, vol. 169, p. 112829, 2024, doi: 10.1016/j.ecolind.2024.112829.

18. R. Sun, S. Shi, Y. Reheman, and S. Li, 'Measurement of urban flood resilience using a quantitative model based on the correlation of vulnerability and resilience', International Journal of Disaster Risk Reduction, vol. 82, p. 103344, 2022, doi: 10.1016/j.ijdrr.2022.103344.
19. R. Jerch, M. E. Kahn, and G. C. Lin, 'Local public finance dynamics and hurricane shocks', Journal of Urban Economics, vol. 134, p. 103516, 2023, doi: 10.1016/j.jue.2022.103516.
20. G. Di Baldassarre et al., 'Hess Opinions: An interdisciplinary research agenda to explore the unintended consequences of structural flood protection', Hydrology and Earth System Sciences, vol. 22, no. 11, pp. 5629–5637, 2018, doi: 10.5194/hess-22-5629-2018.
21. M. Mabrouk, H. Han, M. G. N. Mahran, K. I. Abdrabo, and A. Yousry, 'Revisiting urban resilience: a systematic review of multiple-scale urban form indicators in flood resilience assessment', Sustainability, vol. 16, no. 12, p. 5076, 2024, doi: 10.3390/su16125076.
22. R. J. Klein et al., 'Climate change 2014: impacts, adaptation, and vulnerability', IPCC fifth assessment report, Stockholm, Sweden, 2014.
23. A. K. Jha, R. Bloch, and J. Lamond, Cities and flooding: a guide to integrated urban flood risk management for the 21st century. World Bank Publications, 2012.
24. C. Clar, L. Löschner, R. Nordbeck, T. Fischer, and T. Thaler, 'Population dynamics and natural hazard risk management: conceptual and practical linkages for the case of Austrian policy making', Natural hazards, vol. 105, no. 2, pp. 1765–1796, 2021, doi: 10.1007/s11069-020-04376-z.
25. S. Zhang, J. Cai, Y. Wei, Q. Yang, and L. Li, 'Characteristics of urban network and city functions in the Yangtze River Delta Region: A multi-scale perspective', Heliyon, vol. 10, no. 9, 2024, doi: 10.1016/j.heliyon.2024.e30377.
26. X. Wu, S. Yang, S. Yin, and H. Xu, 'Spatial-temporal dynamic characteristics and its driving mechanism of urban built-up area in Yangtze River Delta based on GTWR model', Resour. Environ. Yangtze Basin, vol. 30, no. 11, pp. 2594–2606, 2021.
27. Z. C. Zhou and J. Wang, 'Evolution of landscape dynamics in the Yangtze River Delta from 2000 to 2020', Journal of Water and Climate Change, vol. 13, no. 3, pp. 1241–1256, 2022, doi: 10.2166/wcc.2022.307.
28. State Council of the People's Republic of China, 'Outline of the Regional Integrated Development Plan for the Yangtze River Delta', 2019. [Online]. Available: https://www.gov.cn/zhengce/202203/content_3635428.htm
29. Intergovernmental Panel on Climate Change (IPCC), 'Climate Change 2022: Impacts, Adaptation and Vulnerability', 2022. [Online]. Available: https://www.ipcc.ch/report/ar6/wg2/?utm_source=chatgpt.com
30. Q. Wang, H. Gu, X. Zang, M. Zuo, and H. Li, 'Flood resilience in cities and urban agglomerations: a systematic review of hazard causes, assessment frameworks, and recovery strategies based on LLM tools', Natural Hazards, pp. 1–36, 2025.
31. C. E. Shannon, 'A mathematical theory of communication', The Bell system technical journal, vol. 27, no. 3, pp. 379–423, 1948, doi: 10.1002/j.1538-7305.1948.tb01338.x.
32. Z. Wang, X. Xu, and J. Zhang, 'Spatial spillover and threshold effect of green development efficiency on urban human settlement resilience in Yangtze River Delta urban agglomeration', Plos one, vol. 18, no. 10, p. e0292230, 2023, doi: 10.1371/journal.pone.0292230.
33. O. Dewa, D. Makoka, and O. A. Ayo-Yusuf, 'Measuring community flood resilience and associated factors in rural Malawi', Journal of flood risk management, vol. 16, no. 1, p. e12874, 2023, doi: 10.1111/jfr3.12874.
34. R. M. Baron and D. A. Kenny, 'The moderator–mediator variable distinction in social psychological research: Conceptual, strategic, and statistical considerations.', Journal of personality and social psychology, vol. 51, no. 6, p. 1173, 1986, doi: 10.1037/0022-3514.51.6.1173.
35. M. Saisana, A. Saltelli, and S. Tarantola, 'Uncertainty and sensitivity analysis techniques as tools for the quality assessment of composite indicators', Journal of the Royal Statistical Society Series A: Statistics in Society, vol. 168, no. 2, pp. 307–323, 2005, doi: 10.1111/j.1467-985X.2005.00350.x.
36. W. McKinney and others, 'Data structures for statistical computing in Python', scipy, vol. 445, no. 1, pp. 51–56, 2010.
37. J. R. Taylor, An introduction to error analysis: the study of uncertainties in physical measurements. MIT Press, 2022.

38. E. A. Drost, 'Validity and reliability in social science research', Education Research and perspectives, vol. 38, no. 1, pp. 105–123, 2011, doi: 10.70953/ERPv38.11005.
39. N. Zhao and Z. Bai, 'Analysis of rounded data in measurement error regression', Journal of the Korean Statistical Society, vol. 42, no. 3, pp. 415–429, 2013, doi: 10.1016/j.jkss.2013.01.003.
40. O. Y. Chen et al., 'The roles, challenges, and merits of the p value', Patterns, vol. 4, no. 12, 2023, doi: 10.1016/j.patter.2023.100878.
41. M. Maier and D. Lakens, 'Justify your alpha: A primer on two practical approaches', Advances in Methods and Practices in Psychological Science, vol. 5, no. 2, p. 25152459221080396, 2022, doi: 10.1177/25152459221080396.
42. K. J. Preacher and A. F. Hayes, 'Asymptotic and resampling strategies for assessing and comparing indirect effects in multiple mediator models', Behavior research methods, vol. 40, no. 3, pp. 879–891, 2008, doi: 10.3758/BRM.40.3.879.
43. R. M. O'brien, 'A caution regarding rules of thumb for variance inflation factors', Quality & quantity, vol. 41, no. 5, pp. 673–690, 2007, doi: 10.1007/s11135-006-9018-6.
44. J. F. Hair, Multivariate data analysis, 7th ed. Prentice-Hall, 2009.
45. J. Capuno, J. Corpuz, and S. Lordemus, 'Natural disasters and local government finance: Evidence from Typhoon Haiyan', Journal of Economic Behavior & Organization, vol. 220, pp. 869–887, 2024, doi: 10.1016/j.jebo.2024.03.007.
46. X. Chenhong and Z. Guofang, 'The spatiotemporal evolution pattern of urban resilience in the Yangtze River Delta urban agglomeration based on TOPSIS-PSO-ELM', Sustainable Cities and Society, vol. 87, p. 104223, 2022, doi: 10.1016/j.scs.2022.104223.
47. Y. Li, J. Zheng, F. Li, X. Jin, and C. Xu, 'Assessment of municipal infrastructure development and its critical influencing factors in urban China: A FA and STIRPAT approach', PloS one, vol. 12, no. 8, p. e0181917, 2017.
48. M. Pregnolato, A. Ford, S. M. Wilkinson, and R. J. Dawson, 'The impact of flooding on road transport: A depth-disruption function', Transportation research part D: transport and environment, vol. 55, pp. 67–81, 2017, doi: 10.1016/j.trd.2017.06.020.
49. M. J. Breen, A. S. Kebede, and C. S. König, 'The safe development paradox in flood risk management: a critical review', Sustainability, vol. 14, no. 24, p. 16955, 2022, doi: 10.3390/su142416955.
50. T. Yang and L. Wang, 'Did Urban Resilience Improve during 2005–2021? Evidence from 31 Chinese Provinces', Land, vol. 13, no. 3, p. 397, 2024, doi: 10.3390/land13030397.
51. S. Davoudi et al., 'Resilience: a bridging concept or a dead end?"Reframing" resilience: challenges for planning theory and practice interacting traps: resilience assessment of a pasture management system in Northern Afghanistan urban resilience: what does it mean in planning practice? Resilience as a useful concept for climate change adaptation? The politics of resilience for planning: a cautionary note: edited by Simin Davoudi and Libby Porter', Planning theory & practice, vol. 13, no. 2, pp. 299–333, 2012, doi: 10.1080/14649357.2012.677124.

APPENDIX A

Table A1 Indicator Data For 41 Cities In Yrd

City	Built-up area (km^2)	Built-up area population density (people/km^2)	GDP density (10,000 RMB/km^2)	Built-up area green coverage rate (%)	Annual average rainfall (mm)	Built-up area drainage pipeline density (km/km^2)	Built-up area road density (km/km^2)	Per capita fiscal revenue (RMB /people)	Hospital beds per 10,000 people
Shanghai	1242.01	3923.00	380179.36	37.83	1414.20	18.21	4.80	33417.76	66
Hangzhou	859.14	8425.06	219511.96	42.81	1171.80	12.18	8.03	67923.75	80
Ningbo	406.51	7775.57	404737.89	43.43	1432.80	18.95	8.03	107061.81	62
Wenzhou	290.94	6141.63	300096.24	45.33	1455.30	11.62	8.49	57294.84	51
Jiaxing	170.79	5862.43	413490.25	42.81	1140.40	11.96	7.46	110122.01	38
Huzhou	142.49	7952.02	281774.16	42.17	1326.00	8.34	8.06	61478.23	96
Shaoxing	267.37	8372.26	291393.95	45.85	1224.10	14.51	8.77	41393.98	88
Jinhua	118.50	18890.21	507257.38	43.51	1340.60	17.24	8.86	38767.65	53
Quzhou	88.34	9638.48	240547.88	43.02	1671.60	25.08	8.35	37729.18	76
Zhoushan	71.73	9906.19	292903.95	45.32	1102.60	16.44	8.21	74575.24	57
Taizhou (Zhejiang)	161.73	10162.38	385890.06	45.32	1251.80	13.09	8.10	50618.11	54
Lishui	50.03	8561.02	392564.46	44.08	1159.30	17.65	6.17	73010.54	166
Hefei	515.00	5096.00	246092.82	46.04	994.70	7.51	6.80	11028.60	93
Huaibei	90.00	3405.00	151724.44	47.00	937.20	5.59	8.22	8214.95	101
Bozhou	77.00	4833.00	287766.23	44.36	933.80	10.39	8.49	7106.66	147
Suzhou (Anhui)	92.00	3803.00	249071.74	45.44	936.20	6.40	9.66	6391.35	155
Bengbu	155.00	2722.00	136511.61	44.81	866.20	4.49	8.74	9237.87	134
Fuyang	156.00	3420.00	213057.05	46.16	944.00	5.78	8.12	5333.49	165
Huainan	128.00	2776.00	125121.88	48.43	768.10	5.85	8.80	6836.70	110
Chuzhou	121.00	2542.00	312562.81	48.28	904.70	9.93	8.74	11519.54	108
Liuan	83.00	3654.00	254627.71	46.30	1215.60	6.70	8.48	7775.49	156
Maanshan	106.00	4688.00	244391.51	47.23	1097.80	6.51	9.46	12918.34	99
Wuhu	266.00	1809.00	178235.71	46.31	1221.90	5.70	8.15	14813.25	98
Xuancheng	77.00	2749.00	253494.81	46.49	1364.20	7.31	8.09	12522.84	113
Tongling	91.00	2041.00	135146.15	44.42	1424.50	10.05	8.66	12822.01	111
Chizhou	51.00	1233.00	218074.51	47.62	1485.80	6.86	9.35	11343.45	116
Anqing	169.00	2501.00	170313.02	43.91	1510.60	6.46	8.14	8177.00	121
Huangshan	71.00	765.00	147366.20	49.95	1609.20	6.11	9.39	10635.51	132
Nanjing	901.00	9239.40	193356.27	45.00	1276.20	12.10	12.09	19459.92	87
Wuxi	584.00	10691.61	264660.79	44.50	1266.00	23.80	7.07	19145.41	60
Xuzhou	509.00	11985.85	174861.30	43.20	954.60	12.50	5.32	8948.99	56
Changzhou	315.00	13396.51	321154.29	44.80	1217.80	25.40	9.19	16121.24	68
Suzhou	776.00	13773.45	317698.07	44.40	1406.80	19.50	9.72	22986.19	33
Nantong	447.00	12579.64	264278.97	44.50	1238.90	12.70	7.93	12095.82	52
Lianyungang	324.00	9074.38	134679.32	43.00	1087.10	15.40	6.27	8707.87	54
Huaian	336.00	9143.15	149257.74	44.60	1226.10	15.70	6.72	10305.98	66
Yancheng	416.00	10655.05	177977.64	39.20	898.10	6.30	4.16	10890.69	39
Yangzhou	312.00	10697.12	237925.00	44.00	1549.30	18.70	6.20	10414.08	50
Zhenjiang	242.00	10757.85	217523.55	43.50	1406.00	10.90	6.48	12318.89	39
Taizhou	281.00	11239.50	239560.85	44.50	1631.40	14.50	5.43	13922.05	41
Suqian	298.00	10857.38	147586.24	45.00	1068.70	14.20	4.25	9333.95	35

Table A2 Exposure (E), Sensitivity (S), Adaptability (A), And Flood Resilience Index (Fri) Across 41 Cities In The Yangtze River Delta (2023)

City	Exposure (E)	Sensitivity (S)	Adaptability (A)	Flood Resilience Index (FRI)
Shanghai	0.4299	0.4587	0.2423	0.2727
Hangzhou	0.5748	0.4299	0.5184	0.5160
Ningbo	0.5099	0.5318	0.7115	0.6831
Wenzhou	0.6690	0.3457	0.4026	0.3967
Jiaxing	0.5925	0.4345	0.6721	0.6544
Huzhou	0.6818	0.2670	0.5136	0.5414
Shaoxing	0.6366	0.5074	0.3893	0.3403
Jinhua	0.2459	0.5174	0.3037	0.3978
Quzhou	0.6984	0.6128	0.3370	0.2570
Zhoushan	0.6464	0.5952	0.5127	0.4129
Taizhou (Zhejiang)	0.5324	0.4539	0.3640	0.3691
Lishui	0.5834	0.5958	0.6989	0.5927
Hefei	0.6932	0.3974	0.1933	0.1772
Huaibei	0.9114	0.3749	0.2136	0.1661
Bozhou	0.7546	0.4782	0.3059	0.2481
Suzhou (Anhui)	0.8096	0.3808	0.3339	0.2805
Bengbu	0.9258	0.3460	0.2952	0.2321
Fuyang	0.8379	0.3688	0.3276	0.2715
Huainan	0.9415	0.4543	0.2317	0.1660
Chuzhou	0.7684	0.5169	0.2541	0.1977
Liuan	0.8093	0.3035	0.3282	0.2949
Maanshan	0.7928	0.3480	0.2537	0.2224
Wuhu	0.8804	0.2745	0.2443	0.2116
Xuancheng	0.8303	0.2719	0.2615	0.2373
Tongling	0.9552	0.3040	0.2664	0.2116
Chizhou	0.9011	0.2307	0.2793	0.2468
Anqing	0.8949	0.1720	0.2537	0.2378
Huangshan	0.9741	0.1933	0.3083	0.2641
Nanjing	0.5739	0.4156	0.3048	0.3080
Wuxi	0.5451	0.7308	0.1772	0.1389
Xuzhou	0.6209	0.5161	0.0845	0.0744
Changzhou	0.4942	0.7936	0.2058	0.1598
Suzhou	0.3889	0.5657	0.1816	0.1903
Nantong	0.5366	0.4392	0.1301	0.1333
Lianyungang	0.7598	0.5478	0.0928	0.0709
Huaian	0.7418	0.5259	0.1318	0.1040
Yancheng	0.6657	0.3249	0.0443	0.0447
Yangzhou	0.6301	0.4916	0.0934	0.0833
Zhenjiang	0.6638	0.3234	0.0847	0.0858
Taizhou	0.6242	0.3554	0.0830	0.0848
Suqian	0.7164	0.5426	0.0273	0.0217